Atmos. Meas. Tech. Discuss., 6, 4577–4605, 2013
www.atmos-meas-tech-discuss.net/6/4577/2013/
doi:10.5194/amtd-6-4577-2013

Atmospheric Measurement Techniques Discussions
Open Access

Validation of the Suomi NPP Ozone Mapping and Profiler Suite total column ozone using Brewer and Dobson spectrophotometers

K. Bai[1,2], C. Liu[1,2], R. Shi[1,2], and W. Gao[1,2,3]

[1]Key Laboratory of Geographic Information Science, Ministry of Education, East China Normal University, Shanghai, China
[2]Joint Laboratory for Environment Remote Sensing and Data Assimilation, East China Normal University, Shanghai, China
[3]Department of Ecosystem Science and Sustainability, Colorado State University, Fort Collins, CO, USA

Received: 30 April 2013 – Accepted: 9 May 2013 – Published: 23 May 2013

Correspondence to: K. Bai (kaixubai@gmail.com)

Published by Copernicus Publications on behalf of the European Geosciences Union.

Abstract

This study mainly focuses on the validation of total column (TC) ozone data derived from the Ozone Mapping and Profiler Suite (OMPS) on board the NASA's Suomi National Polar-orbiting Partnership satellite (NPP). OMPS is an advanced suite of three hyperspectral instruments that maps global ozone on a daily basis and extends the more than 30 yr total ozone and ozone profile records. The algorithm used to derive OMPS TC ozone is adapted from the heritage of Total Ozone Mapping Spectrometer (TOMS) Version 7 algorithm but with a number of enhancements. Validation is primarily performed through comparisons with an ensemble of 74 global distributed Brewer and Dobson spectrophotometers measurements. Linear regression performs fair agreement between OMPS TC ozone and ground-based TC ozone measurements with root mean square error (RMSE) around of 3 % (10 DU). Comparison shows that OMPS TC ozone estimates 0.21 % higher than Brewer measurements average, with station-to-station standard deviation of 3.14 %. As comparing with Dobson measurements, OMPS TC ozone averages 0.86 % higher than the station average with standard deviation of 3.05 %. The relative differences between OMPS and ground TC ozone were analysed varying with latitude and time as well as viewing geometry respectively. Comparisons show relative differences within 2 % over most of latitude and viewing conditions. Only comparing with Brewer measurements did it show an OMPS TC ozone dependent error, large negative bias was observed as OMPS TC ozone below 220 DU and positive bias shown above 460 DU.

1 Introduction

Although the total amount makes up only 0.6 parts per million of the Earth's atmosphere composition, as a trace gas, ozone plays an important role in protecting the life on Earth by blocking most of the energetic part of the Sun's high frequency ultraviolet (UV) radiation, which is potentially damaging to the life forms (Antón et al.,

AMTD
6, 4577–4605, 2013
Validation of the Suomi NPP Ozone Mapping and Profiler Suite total ozone
K. Bai et al.

2011; Varotsos et al., 1995). Acting as a major greenhouse gas, ozone absorbs some of the infrared energy emitted by the Earth and it has very strong radiative forcing effects on regional scales, thus ozone layer changes could be closely associated with the regional to global scales climate change and vice versa (Antón et al., 2010; World Meteorological Organization – WMO, 2007).

Since ozone depletion has been observed in the early 1970s and the first sharp ozone decrease observed in 1980s in the lower stratosphere (Crutzen and Arnold, 1986; Stolarski et al., 1986), many scientific research programs have been proposed to monitoring the ozone layer amount and investigating the reason caused this decrease. According to the scientific research, this decrease is mainly ascribed to the photochemical losses related to anthropogenic causes and dynamical factors (e.g. Antón et al., 2011; Cariolle and Déqué, 1986; Farman et al., 1985; Varotsos, 2002). A relevant consequence of the ozone depletion is the increase of harmful UV radiation at the Earth surface, thus taking steps to monitor the ozone amount in the ozone layer and analyse its variability with high accuracy has been becoming a major issue to protect the ozone layer.

Traditional ground-based spectrophotometers to measure the total ozone amount, such as Brewer and Dobson, although they can provide daily ozone measurements with high accuracy, the spatial coverage limitations of them are obviously. In this context, satellite instruments that measure TC ozone with high spatial and temporal resolutions have been becoming the main scientific research technique for ozone layer monitoring. To date, many instruments specifically designed for TC ozone and ozone profile monitoring have been launched into space, such as the Solar Backscatter Ultraviolet (SBUV and SBUV/2) (Bhartia et al., 2012; Flynn et al., 2009), Total Ozone Mapping Spectrometer (TOMS) (McPeters et al., 1996a,b, 1998) and Ozone Monitoring Instrument (OMI) (Levelt et al., 2006). In addition, there are many European missions, including the Scanning Imaging Absorption Spectrometer for Atmospheric Cartography (SCIAMACHY) (Bovensmann et al., 1999) and the Globe Ozone Monitoring Experiment (GOME and GOME-2) (Balis et al., 2007b; Van Roozendael et al.,

AMTD
6, 4577–4605, 2013

2012). Meanwhile, the Total Ozone Unit (TOU) on board the Chinese FY-3 series satellite is also designed to map global TC ozone on a daily basis (Bai et al., 2013; Wang et al., 2011).

Over the more than 30 yr period, these instruments have provided a very detailed and important long-term record of the global distribution of ozone. OMPS, the Ozone Mapping and Profiler Suite, on board the Suomi National Polar-orbiting Partnership satellite launched on 28 October 2011, carries on this long tradition of space borne ozone measurements beginning in the 1970s and will continue the program for monitoring the Earth's ozone layer in the coming years. These ozone records, which have been used by the ozone-assessment researchers and policy makers to track the health of the ozone layer, thus, the quality of TC ozone derived from space borne instruments, should be first examined to evaluate its accuracy and check whether it meets the requirements.

The main objective of this study is to report the quality and accuracy of the 14 months TC ozone products derived from the OMPS observations since it was launched. Validation activities were performed through comparisons between the OMPS TC ozone data and co-located ground-based Brewer and Dobson spectrophotometers TC ozone measurements. Discrepancies between the OMPS TC ozone and corresponding ground-based measurements were analysed varying with latitude and viewing conditions, and the possible reasons were also examined.

The article is organized as follows. Section 2 describes the instrument and data records used for the validation process. Section 3 presents the detail validation process against ground-based measurements and the conclusions are summarized in Sect. 4.

2 Instruments and measurements

In this section, the instruments to measure TC ozone used in this study will be described separately. The OMPS instruments and the algorithm to derive TC ozone from

AMTD
6, 4577–4605, 2013

OMPS observations are introduced in Sect. 2.1, and the ground Brewer and Dobson measurements are described in Sect. 2.2.

2.1 OMPS observations

2.1.1 OMPS system

OMPS, an important component of the National Polar-Orbiting Operational Environmental Satellite System (NPOESS) flying on Suomi NPP, is the latest of a series of space borne ozone mapping instruments. It is designed to describe the vertical, horizontal, and temporal distribution of ozone in the Earth's atmosphere on a daily basis and then answer the scientific question of whether the ozone layer is recovering as expected after the sharp decrease of ozone in the 1980s.

OMPS is an advanced suite of three hyper spectral instruments that measure sunlight in the ultraviolet and visible backscattered from the Earth's atmosphere. The system consists of a nadir mapper that maps global ozone with about 50 km ground resolution, a nadir profiler that measures the vertical distribution of ozone in the stratosphere, and a limb profiler that measures ozone in the lower stratosphere and troposphere with high resolution (Dittman et al., 2002).

The detectors of OMPS system are two-dimensional Charge-Coupled Devices (CCD) focal plane arrays (FPA), each arranged with one spectral and one spatial dimension. The nadir total column sensor uses a single grating and a CCD array detector to measure backscattered radiance every 0.4 nm from 300 to 380 nm with 1 nm full-width half maximum (FWHM) spectral resolution. It has a 110° cross-track Field-of-View (FOV) and 0.27° along-track slit width. The measurements from cross-track are combined into 35 bins as 3.35° (50 km) at nadir and 2.84° at ±55°. The along-track resolution is 50 km at nadir for mapping TC ozone across a 2800 km swath with a 7.6 s reporting period (Flynn et al., 2004).

The nadir profiler employs a double monochromator and a CCD array detector to make measurements every 0.4 nm from 250 to 310 nm with 1 nm FWHM resolution. It

AMTD
6, 4577–4605, 2013

has a 16° cross-track FOV and 0.26° along-track slit width. The reporting period is 38 s forming a 250 km × 250 km cell size synchronized with five Nadir Mapper cells.

For the NPP mission, the OMPS also contains a limb system that has a focal plane operating from 290 to 1000 nm for high vertical resolution ozone profile observations. It has three vertical slits separated by 4.25° across track with a 19 s reporting period equates to 125 km along-track motion. Each slit has a vertical FOVs of 1.95° corresponding to 112 km equating to 0 to 60 km coverage at the limb, plus offsets for pointing uncertainty, orbital variation, and Earth oblateness (Flynn et al., 2004).

2.1.2 Nadir total ozone measurements

The NPP ground processing system receives and processes the sensor data into Raw Data Records (RDRs), Sensor Data Records (SDRs) and Environmental Data Records (EDRs) or Intermediate Products (IPs). In this study, the TC ozone from the daily granule nadir EDRs for the period of January 2012 to February 2013 were employed for the comparisons with ground-based measurements. The TC ozone EDRs were acquired from the Ozone and Air Quality archive sets available from NASA Goddard Space Flight Center (http://ozoneaq.gsfc.nasa.gov/beta/data/omps/). Thus, the algorithm to derive OMPS TC ozone will be only discussed here.

The nadir total column EDR product consists of the total ozone in a column of air from 0 to 60 km and observed for all solar zenith angle (SZA) viewing conditions less than or equal to 80°. The algorithm is adapted from the TOMS Version 7 algorithm (McPeters et al., 1996a) but with several enhancements to take advantage of the high spectral resolution. The OMPS algorithm estimates the TC ozone based on the comparison of measured normalized radiance to calculated normalized radiance by using a standard UV radiative transfer model for different ozone amount, specific measurement geometry, viewing conditions and surface conditions. The algorithm uses multiple triplets of measurements. The triplets combine an ozone insensitive channel (at 360 or 380 nm) that provides description of cloud fraction and reflectivity, with a pair of channels at ozone absorption bands. The pairs are selected as one chosen for the ozone

AMTD
6, 4577–4605, 2013

strongly absorption channels, which are usually placed at 308.5, 310.5, 312.2, 314.0, 315.0, 316.0, 317.0, 318.0, 320.0, 322.5, 325.0, 328.0, or 331.0 nm. These channels are paired with weaker absorption channels of 321.0, 329.0, 332.0, or 336.0 nm (Flynn et al., 2004). The detail description of scientific basis of ozone retrieval from backscattered UV irradiance has been reported in many articles (e.g. Dave and Mateer, 1967; McPeters et al., 1996a, 1998; Rodriguez et al., 2003).

The OMPS TC ozone retrieval starts out by the calculation of an effective cloud fraction. The effective cloud fraction can be derived by comparing the measured radiance at an ozone insensitive wavelength with one calculated for cloud and for ground reflection. Given this calculated effective cloud fraction and the radiance measured at a pair of wavelengths (one strongly absorbed by ozone as another weakly), an initial ozone estimate can be derived by interpolation of the normalized radiance as a function of ozone using the viewing conditions of the measurement.

After an initial ozone estimate is calculated, a linear correction that accounts for differences between the Rayleigh scattering atmosphere model assumed in computing the look-up tables and the actual atmosphere measured by the sensor will then be applied to this initial ozone. According to Baker and Kilcoyne (2011), this linear correction will overcorrect the total ozone estimate in the presence of the tropospheric aerosols or for the case of sun glint, and then a second adjustment based on the 331–376 nm residue difference is applied to the ozone value estimated above effectively.

In order to minimize the errors of the total ozone amount derived from the OMPS measurements, many useful enhancements processes have been proposed, such as using the climatological values of tropospheric ozone amount along with layer ozone sensitivities to correct the tropospheric ozone, using multiple sets of triplets and 4 different ozone insensitive wavelengths to derive reflectivity to reduce the errors due to sensor noise. After these similar refinements from aerosols and other contaminants, the nadir TC ozone EDRs is constructed (Baker and Kilcoyne, 2011).

2.2 Ground-based measurements

To date, the worldwide, well-established ground-based network of Brewer and Dobson spectrophotometers, has been generally considered as the ground-truth of total ozone monitoring (Antón et al., 2010; Bai et al., 2013). Over the past decades, TC ozone measured from these two spectrophotometers has been widely used to validate the space borne instruments due to its high accuracy. The working principles and scientific basis of these two spectrophotometers have been described in many scientific papers, see e.g. Bernhard (2005); Brewer (1973); Dobson (1968); Kerr (2002) and Van Roozendael et al. (1998) for detail description.

A well-maintained and calibrated Dobson instrument measures total ozone with an estimated accuracy of 1 % for direct sun and 2–3 % for zenith sky or for SZAs less than 75° (Basher, 1982). A well-calibrated Brewer instrument has an error level comparable to the Dobson instrument, with a precision of 1 % over long time intervals (Antón et al., 2009b). Despite the similarity in performance between the Brewer and Dobson instruments, small differences (within ±0.6 %) are still seen due to the use of different wavelengths and varying temperature dependence for the ozone absorption coefficients (Van Roozendael et al., 1998).

In this study, TC ozone measurements recorded from well-maintained 35 Brewer and 39 Dobson spectrophotometers, for the period of January 2012 to February 2013, available from the World Ozone and Ultraviolet Data Centre (WOUDC) archive (http://www.woudc.org), were employed as ground reference to validate the TC ozone derived from the nadir OMPS TC ozone algorithm. The ground stations of Brewer and Dobson are listed in Tables 1 and 2, respectively. In order to obtain a complete evaluation, all direct-sun and zenith sky ground-based total ozone measurements were included.

AMTD
6, 4577–4605, 2013

3 Validation against ground-based measurements

Discrepancies between overpass (distance between ground stations and collocated satellite pixel less than 30 km) nadir OMPS TC ozone records and ground-based measurements were analysed separately using the Brewer and Dobson data sets. Except the spatial and temporal inconsistency between satellite instrument and ground measurements caused error, the latitudinal dependence of these bias error, as well as the dependence on other parameters, such as SZA and radiative cloud fraction, was analysed. The relative differences (RDs) and mean bias error (MBE) between ground-based total ozone measurements and collocated OMPS TC ozone were calculated by the following equation

$$\mathrm{RDs} = 100 \times \frac{\mathrm{OMPS} - \mathrm{Ground}}{\mathrm{OMPS}} \tag{1}$$

$$\mathrm{MBE} = \frac{1}{N} \sum \mathrm{RD}_i \tag{2}$$

where OMPS denotes nadir OMPS TC ozone, Ground denotes ground-based TC ozone measurements, N is the total number of data pairs. Uncertainties regard to MBE is characterized by the standard deviation of the RDs.

To analyse the consistency of OMPS TC ozone and ground station measurements, linear regressions between them are performed as scatter plots shown in Fig. 1 and the statistical parameters retrieved from the regressions presented in Table 3. It shows perfect agreements between OMPS TC ozone and both ground measurements, with R^2 of 0.96 and RMSE of 3.15 % (10 DU), which reveal a high degree of proportionality with little spread. Result shows that the OMPS TC ozone overestimates both ground measurements as Brewer of 0.213 % and Dobson of 0.861 %, with a standard deviation of about 3.1 %. Totally, the OMPS TC ozone agrees better with Dobson than Brewer measurements in spite of larger MBE. This differences are possibly ascribed to the different measure principles of two spectrophotometers (Kerr et al., 1988). In addition,

AMTD
6, 4577–4605, 2013

the frequency count of RDs, as shown in Fig. 2, also demonstrates fair agreements as most of the RDs distributes within ±2 %.

Figure 3 shows the distribution of the bias error between OMPS TC ozone and ground TC ozone measurements as a function of latitude. All the latitudinal MBE is within 2 % comparing with both measurements. Comparing with Brewer measurements, large positive bias is observed near equator with MBE of 1.5 % ± 2.1 % as negative bias observed over Antarctic with MBE of −1.8 % ± 2.8 %. Over other latitude belts, the MBE is within 1 %. Large spread is observed over mid-to-high latitudes in the Northern Hemisphere, with the largest standard deviation of 3.4 % over the 60–70° N belt. As compared to Dobson, OMPS almost overestimated Dobson TC ozone measurements over all latitudes except for 20–30° S and 10–20° N regions. Large positive bias of about 1.7 % presents over mid-latitudes for both hemisphere but with larger uncertainty (3.1 %) in the Northern Hemisphere. However, the largest uncertainty of 3.9 % is observed over the southern high latitude belt (70–80° S). This effect is mainly associated with little reliable measurements over these regions due to bad viewing conditions.

Time series of the monthly MBE were analysed to evaluate the stability of the OMPS TC ozone, as presents in Fig. 4. Similarly, the MBE is observed within 2 % for both measurements as the largest bias of −1.9 % performs in December for OMPS-Brewer comparisons. However, different patterns are observed for both comparisons. As for OMPS-Brewer comparisons, OMPS overestimated Brewer TC ozone during the first ten months and then underestimated. Large bias of about −1.9 % ± 3.6 % (−5 ± 12 DU) is shown during winter season (December to February), and this effect could be associated with the large SZAs during this season for that most of the Brewer instruments used in this study are located in the mid-to-high latitudes in the Northern Hemisphere. Comparing with Dobson measurements, OMPS overestimated TC ozone for all months, and bias varies smoother than comparing with Brewer as demonstrated by the standard deviation. Nevertheless, bias varies larger as is observed since October 2012, which is also shown in OMPS-Brewer comparisons. However, whether this effect

AMTD
6, 4577–4605, 2013

shows the degradation of OMPS instrument or it was caused by other factors, such as SZAs, cannot be asserted here due to limited time series of OMPS TC ozone data.

Figure 5 presents the MBE variation as a function of SZAs. As mentioned above, SZAs will introduce error into satellite observations. Similar patterns are observed from OMPS-Brewer comparisons as MBE varies with SZAs and time. Large negative bias is observed as SZAs above 65°. However, comparing with Dobson measurements, no significant SZAs dependence error is observed. The MBE varies between 0 to 1.3 % as SZAs change from 0 to 90°. This effect is consistent with some former studies, which have shown a small or even no significant dependence on SZAs in comparison between OMI-TOMS TC ozone and ground measurements under all sky conditions (Antón et al., 2009a; Balis et al., 2007a). Meanwhile, the bias error varying with viewing zenith angles (VZAs) is also presented, which is shown in Fig. 6. For both comparisons, no VZAs dependent error is observed as VZAs less than 45°. Nevertheless, large bias error (∼ 1.5 %) performs as VZAs above that. It shows a small dependence bias error that it varies from 0.1 to 1.5 % as VZAs change from 45 to 65° comparing with Brewer measurements. In contrast, no such obvious variation is observed for OMPS–Dobson comparisons.

The bias error, varying with cloud fraction, is shown in Fig. 7. Results show that no cloud dependent error is observed as clouds less than 65 % for both comparisons, with a bias of about 0.6 % for Brewer and 1.2 % for Dobson. As clouds higher than 65 %, OMPS shows a cloud dependent bias error for both ground TC ozone measurements. More clouds present, more significant underestimation is observed. The bias error reaches 1.6 % as clouds present around 95 %. Due to clouds contamination, the sensor can only derive the ozone amount above the cloud with confidence since the satellite sensor is only sensitive to the amount of ozone above the cloud, the ozone amount below the cloud height must be inferred from climatological tables (McPeters et al., 2008).

Figure 8 shows the variability of bias error as a function of reflectivity. In this study, the reflectivity derived from 311 nm measurements of OMPS is employed. It shows

AMTD
6, 4577–4605, 2013

smooth positive bias (0.5 % of Brewer and 1.2 % of Dobson) as reflectivity less than 0.5. However, negative dependent bias is observed as reflectivity varies from 0.5 to 1.0, the largest negative error presents as reflectivity of about 0.85. Meanwhile, the variation in MBE between OMPS TC ozone and ground-based measurements, as a function of OMPS TC ozone value, is shown in Fig. 9. Comparing with Brewer measurements, it shows a significant TC ozone value dependent bias error. Large negative bias (about −4.6 %) is observed as OMPS TC ozone less than 220 DU, which is usually considered as the ozone level of ozone hole. Under this condition, ozone is always measured with large SZAs, and many other errors will be introduced into the long viewing limb. By contrast, large positive bias error (about 3.6 %) is observed as TC ozone higher than 460 DU, and this effect is related to the ground instruments' signal-to-noise limits, which will fail under very high-ozone conditions due to less ground-measurable UV radiation penetrates the atmosphere (Antón et al., 2010).

4 Conclusions and discussion

On the basis of 14 months TC ozone records, the performance of nadir OMPS TC ozone EDRs has been evaluated and we conclude that OMPS TC ozone compares very well with collocated ground-based measurements from the network of worldwide well-maintained Brewer and Dobson spectrophotometers. Comparisons with 35 Brewer and 39 Dobson ground stations show that OMPS TC ozone overestimates 0.21 % higher than Brewer measurements averages with station-to-station standard deviation of 3.14 % and averages 0.86 % higher than Dobson measurements with standard deviation of 3.05 %. No significant latitudinal and viewing conditions dependent error is observed except for OMPS–Brewer comparisons as VZAs above 45°. Only the OMPS–Brewer comparisons show an OMPS TC ozone value dependent error that the bias error increases from −4.6 to 3.6 % as the OMPS TC ozone varies from 170 to 550 DU.

Overall, the OMPS TC ozone EDRs product performs very well with an accuracy of mean bias error less than 1 %, and it can be used with confidence for global ozone

AMTD
6, 4577–4605, 2013

monitoring and other atmospheric applications over most regions of the world. However, due to limited time series of OMPS TC ozone records, the reason for the large bias error during wintertime has not been fully investigated in this study, and we will continue this research in the next work.

Acknowledgements. This work was partly supported by the National Basic Research Program of China (Grant No. 2010CB951603), the Shanghai Science and Technology Support Program-Special for EXPO (Grant No. 10DZ0581600) and the National Natural Science Foundation of China (41101037). The authors thank the Goddard Earth Sciences Data and Information Services Center, and the World Ozone and Ultraviolet Data Center for their data supports.

References

Antón, M., López, M., Vilaplana, J. M., Kroon, M., McPeters, R., Bañón, M., and Serrano, A.: Validation of OMI-TOMS and OMI-DOAS total ozone column using five Brewer spectroradiometers at the Iberian peninsula, J. Geophys. Res., 114, 1–10, doi:10.1029/2009JD012003, 2009a.

Antón, M., Loyola, D., López, M., Vilaplana, J. M., Bañón, M., Zimmer, W., and Serrano, A.: Comparison of GOME-2/MetOp total ozone data with Brewer spectroradiometer data over the Iberian Peninsula, Ann. Geophys., 27, 1377–1386, doi:10.5194/angeo-27-1377-2009, 2009b.

Antón, M., Koukouli, M. E., Kroon, M., McPeters, R. D., Labow, G. J., Balis, D., and Serrano, A.: Global validation of empirically corrected EP-Total Ozone Mapping Spectrometer (TOMS) total ozone columns using Brewer and Dobson ground-based measurements, J. Geophys. Res., 115, 1–13, doi:10.1029/2010JD014178, 2010.

Antón, M., Bortoli, D., Costa, M. J., Kulkarni, P. S., Domingues, A. F., Barriopedro, D., Serrano, A., and Silva, A. M.: Temporal and spatial variabilities of total ozone column over Portugal, Remote Sens. Environ., 115, 855–863, doi:10.1016/j.rse.2010.11.013, 2011.

Bai, K., Liu, C., Shi, R., Zhang, Y., and Gao, W.: Global validation of FY-3A total ozone unit (TOU) total ozone columns using ground-based Brewer and Dobson measurements, Int. J. Remote Sens., 34, 5228–5242, doi:10.1080/01431161.2013.788264, 2013.

Baker, N. and Kilcoyne, H.: Joint Polar Satellite System (JPSS) OMPS NADIR Total Column Ozone Algorithm Theoretical Basis Document (ATBD), available from: http://npp.gsfc.nasa.gov/science/sciencedocuments/ATBD_122011/474-00029_Rev-Baseline.pdf (last access: 20 December 2012), 2011.

Balis, D., Kroon, M., Koukouli, M. E., Brinksma, E. J., Labow, G., Veefkind, J. P., and McPeters, R. D.: Validation of Ozone Monitoring Instrument total ozone column measurements using Brewer and Dobson spectrophotometer ground-based observations, J. Geophys. Res., 112, 1–10, doi:10.1029/2007JD008796, 2007a.

Balis, D., Lambert, J.-C., Van Roozendael, M., Spurr, R., Loyola, D., Livschitz, Y., Valks, P., Amiridis, V., Gerard, P., Granville, J., and Zehner, C.: Ten years of GOME/ERS2 total ozone data – the new GOME data processor (GDP) version 4: 2. Ground-based validation and comparisons with TOMS V7/V8, J. Geophys. Res., 112, D07307, doi:10.1029/2005JD006376, 2007b.

Basher, R. E.: Review of the Dobson spectrophotometer and its accuracy, Global Ozone Research and Monitoring Project, Report 13, available from: http://www.esrl.noaa.gov/gmd/ozwv/dobson/papers/report13/report13.html (last access: 22 December 2012), 1982.

Bernhard, G.: Bias in Dobson total ozone measurements at high latitudes due to approximations in calculations of ozone absorption coefficients and air mass, J. Geophys. Res., 110, 1–10, doi:10.1029/2004JD005559, 2005.

Bhartia, P. K., McPeters, R. D., Flynn, L. E., Taylor, S., Kramrova, N. A., Frith, S., Fisher, B., and DeLand, M.: Solar Backscatter UV (SBUV) total ozone and profile algorithm, Atmos. Meas. Tech. Discuss., 5, 5913–5951, doi:10.5194/amtd-5-5913-2012, 2012.

Bovensmann, H., Burrows, J. P., Buchwitz, M., Frerick, J., Noël, S., Rozanov, V. V., Chance, K. V., and Goede, A. P. H.: SCIAMACHY: Mission Objectives and Measurement Modes, J. Atmos. Sci., 56, 127–150, doi:10.1175/1520-0469(1999)056<0127:SMOAMM>2.0.CO;2, 1999.

Brewer, A. W.: A replacement for the Dobson spectrophotometer, Pure Appl. Geophys., 106–108, 919–927, doi:10.1007/BF00881042, 1973.

Cariolle, D. and Déqué, M.: Southern Hemisphere medium-scale waves and total ozone disturbances in a spectral general circulation model, J. Geophys. Res., 91, D10825, doi:10.1029/JD091iD10p10825, 1986.

AMTD
6, 4577–4605, 2013

Validation of the Suomi NPP Ozone Mapping and Profiler Suite total ozone

K. Bai et al.

Crutzen, P. J. and Arnold, F.: Nitric acid cloud formation in the cold Antarctic stratosphere: a major cause for the springtime “ozone hole”, Nature, 324, 651–655, doi:10.1038/324651a0, 1986.

Dave, J. and Mateer, C.: A preliminary study on the possibility of estimating total atmospheric ozone from satellite measurements, J. Atmos. Sci., 24, 414–427, doi:10.1175/1520-0469(1967)024<0414:APSOTP>2.0.CO;2, 1967.

Dittman, M. G., Ramberg, E., Chrisp, M., Rodriguez, J. V., Sparks, A. L., Zaun, N. H., Hendershot, P., Dixon, T., Philbrick, R. H., and Wasinger, D.: Nadir ultraviolet imaging spectrometer for the NPOESS Ozone Mapping and Profiler Suite (OMPS), in: Proceedings of SPIE 4814, Earth Observing Systems VII, 25 September 2002, Seattle, WA, edited by: Barnes, W. L., 111–119, 2002.

Dobson, G. M. B.: Forty years’ research on atmospheric ozone at Oxford: a history, Appl. Optics, 7, 387–405, doi:10.1364/AO.7.000387, 1968.

Farman, J. C., Gardiner, B. G., and Shanklin, J. D.: Large losses of total ozone in Antarctica reveal seasonal ClO_x/NO_x interaction, Nature, 315, 207–210, doi:10.1038/315207a0, 1985.

Flynn, L., Hornstein, J., and Hilsenrath, E.: The ozone mapping and profiler suite (OMPS), in: IEEE International Geoscience and Remote Sensing Symposium, 2004, IGARSS’04 Proceedings 2004, vol. 1, 152–155, 2004.

Flynn, L. E., McNamara, D., Beck, C. T., Petropavlovskikh, I., Beach, E., Pachepsky, Y., Li, Y. P., Deland, M., Huang, L.-K., Long, C. S., Tiruchirapalli, R., and Taylor, S.: Measurements and products from the Solar Backscatter Ultraviolet (SBUV/2) and Ozone Mapping and Profiler Suite (OMPS) instruments, Int. J. Remote Sens., 30, 4259–4272, doi:10.1080/01431160902825040, 2009.

Kerr, J. B.: New methodology for deriving total ozone and other atmospheric variables from Brewer spectrophotometer direct sun spectra, J. Geophys. Res., 107, 1–17, doi:10.1029/2001JD001227, 2002.

Kerr, J. B., Asbridge, I. A., and Evans, W. F. J.: Intercomparison of total ozone measured by the Brewer and Dobson spectrophotometers at Toronto, J. Geophys. Res., 93, 11129, doi:10.1029/JD093iD09p11129, 1988.

Levelt, P. F., Van den Oord, G. H. J., Dobber, M. R., Malkki, A., Stammes, P., Lundell, J. O. V., and Saari, H.: The ozone monitoring instrument, IEEE T. Geosci. Remote, 44, 1093–1101, doi:10.1109/TGRS.2006.872333, 2006.

AMTD

6, 4577–4605, 2013

McPeters, R. D., Bhartia, P. K., Krueger, A. J., Herman, J. R., Schlesinger, B. M., Wellemeyer, C. G., Seftor, C. J., Jaross, G., Taylor, S. L., Swissler, T., Torres, O., Labow, G., Byerly, W., and Cebula, R. P.: Nimbus-7 Total Ozone Mapping Spectrometer (TOMS) data products user's guide, available at: http://macuv.gsfc.nasa.gov/doc/n7usrguide.pdf, last access: 21 November 2012, 1996a.

McPeters, R. D., Hollandsworth, S. M., Flynn, L. E., Herman, J. R., and Seftor, C. J.: Long-term ozone trends derived from the 16 year combined Nimbus 7/Meteor 3 TOMS Version 7 record, Geophys. Res. Lett., 23, 3699, doi:10.1029/96GL03540, 1996b.

McPeters, R. D., Bhartia, P. K., Krueger, A. J., Herman, J. R., Wellemeyer, C. G., Seftor, C. J., Jaross, G., Torres, O., Moy, L., Labow, G., Byerly, W., Taylor, S. L., Swissler, T., and Cebula, R. P.: Earth Probe Total Ozone Mapping Spectrometer (TOMS) Data Products User's Guide, NASA Reference Publication, Greenbelt, Maryland, 1998.

McPeters, R., Kroon, M., Labow, G., Brinksma, E., Balis, D., Petropavlovskikh, I., Veefkind, J. P., Bhartia, P. K., and Levelt, P. F.: Validation of the Aura Ozone Monitoring Instrument total column ozone product, J. Geophys. Res., 113, D15S14, doi:10.1029/2007JD008802, 2008.

Rodriguez, J. V., Seftor, C. J., Wellemeyer, C. G., and Chance, K.: An overview of the Nadir sensor and algorithms for the NPOESS Ozone Mapping and Profiler Suite (OMPS), in: Proceedings of SPIE 4891, Optical Remote Sensing of the Atmosphere and Clouds III, Hangzhou, China, edited by: Huang, H.-L., Lu, D., and Sasano, Y., 65–75, 2003.

Stolarski, R. S., Krueger, A. J., Schoeberl, M. R., McPeters, R. D., Newman, P. A., and Alpert, J. C.: Nimbus 7 satellite measurements of the springtime Antarctic ozone decrease, Nature, 322, 808–811, doi:10.1038/322808a0, 1986.

Van Roozendael, M., Peeters, P., Roscoe, H. K., De Backer, H., Jones, A. E., Bartlett, L., Vaughan, G., Goutail, F., Pommereau, J.-P., Kyro, E., Wahlstrom, C., Braathen, G., and Simon, P. C.: Validation of Ground-Based Visible Measurements of Total Ozone by Comparison with Dobson and Brewer Spectrophotometers, J. Atmos. Chem., 29, 55–83, doi:10.1023/A:1005815902581, 1998.

Van Roozendael, M., Spurr, R., Loyola, D., Lerot, C., Balis, D., Lambert, J.-C., Zimmer, W., Van Gent, J., Van Geffen, J., Koukouli, M., Granville, J., Doicu, A., Fayt, C., and Zehner, C.: Sixteen years of GOME/ERS-2 total ozone data: the new direct-fitting GOME Data Processor (GDP) version 5 – algorithm description, J. Geophys. Res., 117, 1–18, doi:10.1029/2011JD016471, 2012.

Varotsos, C. A.: The Southern Hemisphere ozone hole split in 2002, Environ. Sci. Pollut. R., 9, 375–376, doi:10.1007/BF02987584, 2002.
Varotsos, C. A., Chronopoulos, G. J., Katsikis, S., and Sakellariou, N. K.: Further evidence of the role of air pollution on solar ultraviolet radiation reaching the ground, Int. J. Remote Sens., 16, 1883–1886, doi:10.1080/01431169508954525, 1995.
Wang, W., Zhang, X., Wang, Y., Wang, Y., Zhang, Z., Fu, L., Jiang, F., and Liu, G.: Introduction to the FY-3A Total Ozone Unit: instrument, performance and results, Int. J. Remote Sens., 32, 4749–4758, doi:10.1080/01431161.2010.489073, 2011.
WMO – World Meteorological Organization: Scientific Assessment of Ozone Depletion: 2006, Global Ozone Research and Monitoring Project-Report No. 50, Geneva, Switzerland, 572 pp., 2007.

AMTD
6, 4577–4605, 2013

Validation of the Suomi NPP Ozone Mapping and Profiler Suite total ozone

K. Bai et al.

Table 1. List of 35 ground-based Brewer stations selected for comparisons with OMPS total ozone data sets.

STN ID	NAME	LAT. (deg.)	LON. (deg.)	ELEV. (m)	COUNTRY
111	Amundsen-Scott	−89.99	−24.8	2810	Austria
499	Princess	−71.95	23.35	1350	Austria
322	Petaling Jaya	3.102	101.645	86	Malaysia
002	Tamanrasset	22.8	5.5	1384	Algeria
349	Lhasa	29.67	91.13	3650	China
332	Pohang	36	129.4	5	Korea
295	Mt. Waliguan	36.287	100.9	3816	China
213	El Arenosillo	37.1	−6.73	41	Spain
346	Murcia	38	−1.16	69	Spain
348	Ankara	39.97	32.863	913	Turkey
308	Madrid	40.45	−3.717	680	Spain
411	Zaragoza	41.63	−0.89	258	Spain
405	La Coruna	43.33	−8.41	60	Spain
326	Longfengshan	44.73	127.59	334	China
479	Aosta	45.74	7.36	570	Italy
035	Arosa	46.78	9.68	1840	Switzerland
099	Hohenpeissenberg	47.81	11.01	975	Germany
290	Saturna	48.77	−123.13	178	Canada
331	Poprad-Ganovce	49.03	20.32	706	Slovakia
096	Hradec Kralove	50.18	15.83	285	Czech Republic
053	Uccle	50.8	4.35	100	Belgium
353	Reading	51.44	−0.94	66	Great Britain
318	Valentia Observatory	51.93	−10.25	14	Ireland
076	Goose Bay	53.31	−60.36	44	Canada
021	Edmonton	53.55	−114.1	766	Canada
352	Manchester	53.47	−2.23	76	Britain
307	Obninsk	55.12	36.3	100	Russia
279	Norrkoeping	58.58	16.15	43	Sweden
077	Churchill	58.74	−94.07	35	Canada
165	Oslo	59.938	10.717	90	Norway
284	Vindeln	64.24	19.77	225	Sweden
267	Sondrestrom	66.996	−50.621	300	Greenland
024	Resolute	74.72	−94.98	40	Canada
315	Eureka	79.99	−85.93	10	Canada
018	Alert	82.5	−62.4	62	Canada

AMTD
6, 4577–4605, 2013

Table 2. List of 39 ground-based Dobson stations selected for comparisons with OMPS total ozone data sets.

STN ID	NAME	LAT. (deg.)	LON. (deg.)	ELEV. (m)	COUNTRY
057	Halley	−75.36	−26.13	33	Austria
101	Syowa	−69.01	39.58	22	Antarctica
232	Vernadsky	−65.15	−64.16	16	Austria
233	Marambio	−64.23	−56.62	198	Antarctica
339	Ushuaia	−54.85	−68.28	17	Argentina
029	Macquarie Island	−54.5	158.95	10	Australia
091	Buenos Aires	−34.58	−58.48	25	Argentina
159	Perth	−31.92	115.96	2	Australia
340	Springbok	−29.67	17.9	1006	South Africa
027	Brisbane	−27.39	153.13	4	Australia
265	Irene	−25.92	28.217	1523	South Africa
084	Darwin	−12.42	130.89	30	Australia
216	Bangkok	13.67	100.61	53	Thailand
002	Tamanrasset	22.8	5.5	1384	Algeria
311	Havana	23.143	−82.341	50	Cuba
245	Aswan	23.97	32.78	190	Egypt
190	Naha	26.21	127.69	28	Japan
409	Hurghada	27.28	33.75	7	Egypt
014	Tsukuba	36.06	140.13	31	Japan
106	Nashville	36.25	−86.57	182	USA
341	Hanford	36.32	−119.63	73	USA
213	El Arenosillo	37.1	−6.73	41	Spain
208	Xianghe	39.98	116.37	80	China
067	Boulder	40.03	−105.25	1689	USA
410	Amberd	40.38	44.25	2070	Armenia
012	Sapporo	43.06	141.33	26	Japan
065	Toronto	43.781	−79.468	198	Canada
040	Haute Provence	43.93	5.7	684	France
019	Bismarck	46.77	−100.75	511	USA
035	Arosa	46.78	9.68	1840	Switzerland
020	Caribou	46.87	−68.03	192	USA
099	Hohenpeissenberg	47.81	11.01	975	Germany
096	Hradec Kralove	50.18	15.83	285	Czech Republic
498	Kyiv-Goloseyev	50.364	30.497	206	Ukraine
068	Belsk	51.84	20.79	180	Poland
043	Lerwick	60.13	−1.18	82	Great Britain
051	Reykjavik	64.13	−21.9	64	Israel
105	Fairbanks	64.82	−147.87	138	USA
199	Barrow	71.32	−156.6	11	USA

AMTD
6, 4577–4605, 2013

Validation of the Suomi NPP Ozone Mapping and Profiler Suite total ozone

K. Bai et al.

AMTD
6, 4577–4605, 2013

Validation of the Suomi NPP Ozone Mapping and Profiler Suite total ozone

K. Bai et al.

Table 3. Statistics (the number of correlative data points N, the slope of the regression, the coefficient of regression R^2, the root mean square error RMSE and the mean bias error MBE with standard deviation) collected from the comparisons.

	N	Slope	R^2	RMSE %	RMSE DU	MBE (%)
Brewer	8531	0.995	0.956	3.142	10.488	$+0.213 \pm 3.135$
Dobson	6675	0.996	0.963	3.166	9.794	$+0.861 \pm 3.047$

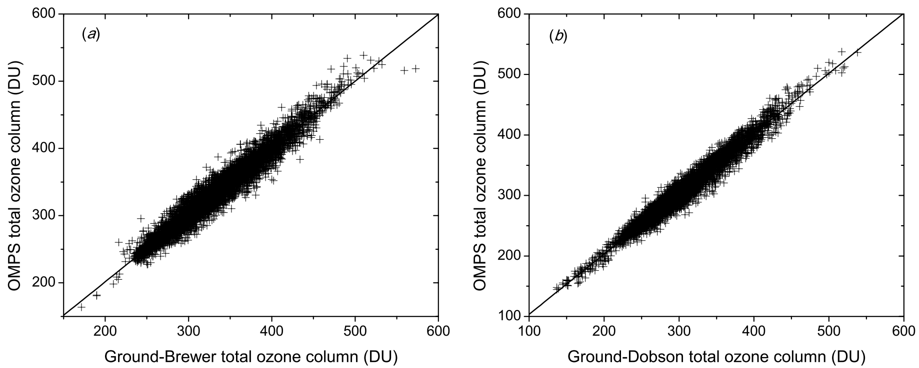

Fig. 1. Scatter plots between OMPS TC ozone and ground-based observations, plotted separately for the Brewer (**a**: $Y = 0.995X + 2.580$, $N = 8531$, $R^2 = 0.956$) and Dobson (**b**: $Y = 0.996X + 4.016$, $N = 6676$, $R^2 = 0.963$).

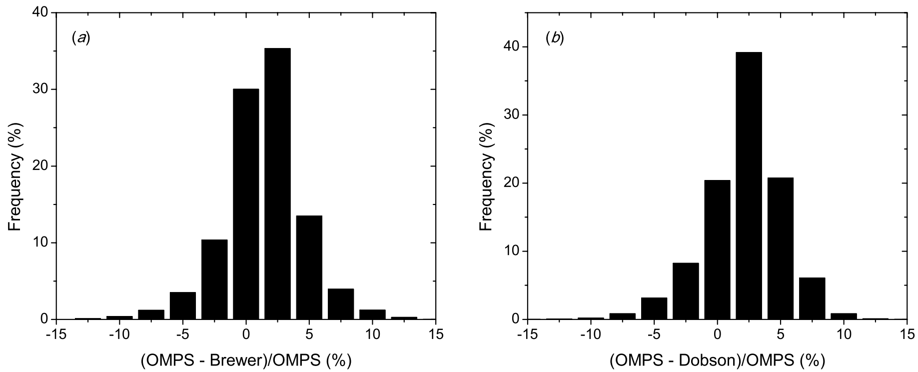

Fig. 2. Frequency statistics of the relative differences between OMPS and Brewer **(a)** as well as Dobson **(b)**.

AMTD
6, 4577–4605, 2013

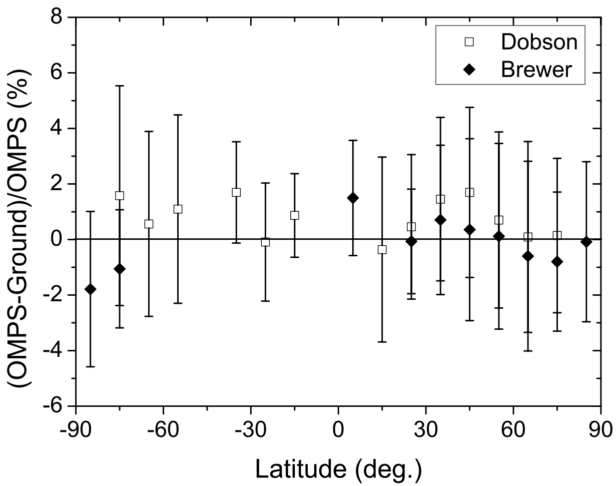

Fig. 3. Mean bias error between OMPS TC ozone and ground measurements as a function of latitude. The ground stations were gathered in 10° latitude bins.

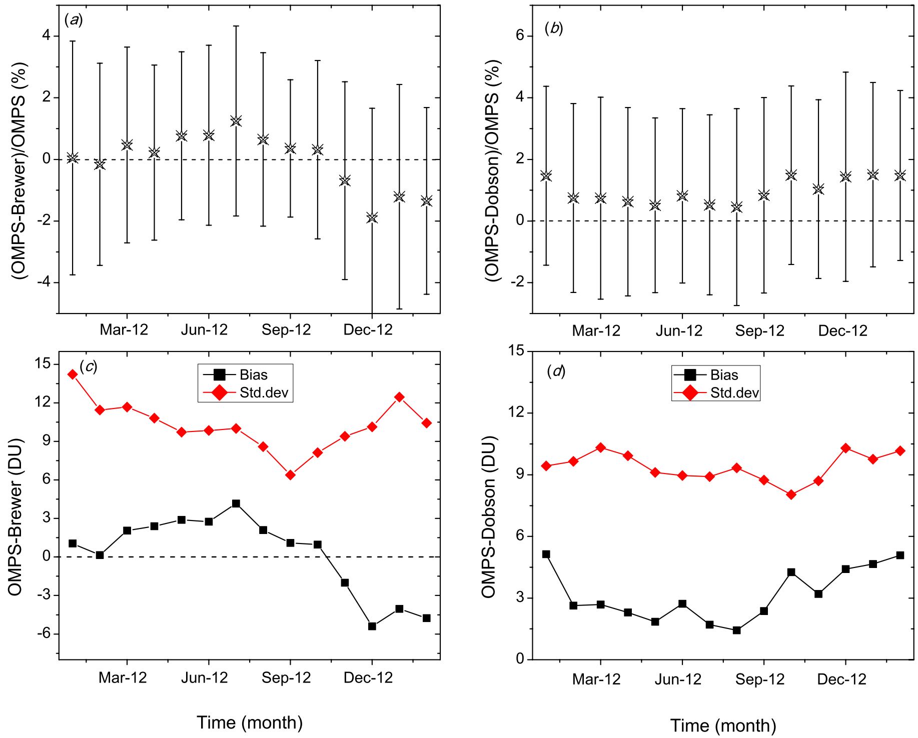

Fig. 4. Monthly mean bias error **(a, b)** and TC ozone differences **(c, d)** versus time.

AMTD
6, 4577–4605, 2013

Title Page
Abstract | Introduction
Conclusions | References
Tables | Figures
◀| |▶
◀ ▶
Back | Close
Full Screen / Esc
Printer-friendly Version
Interactive Discussion

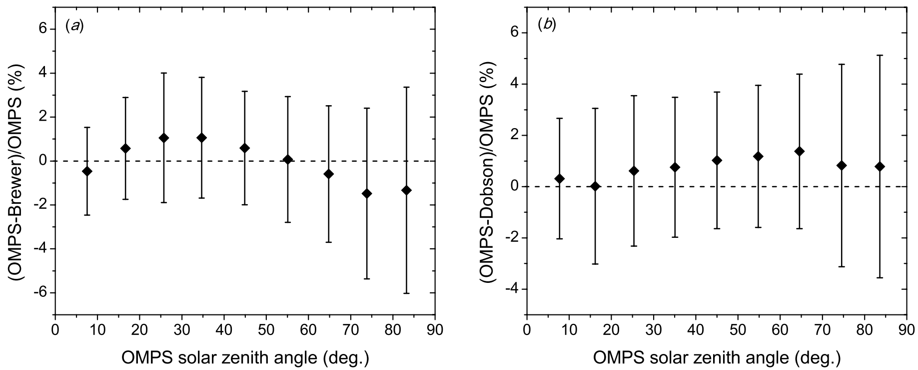

Fig. 5. Investigation of the bias error dependence on OMPS solar zenith angle as binned in 10°.

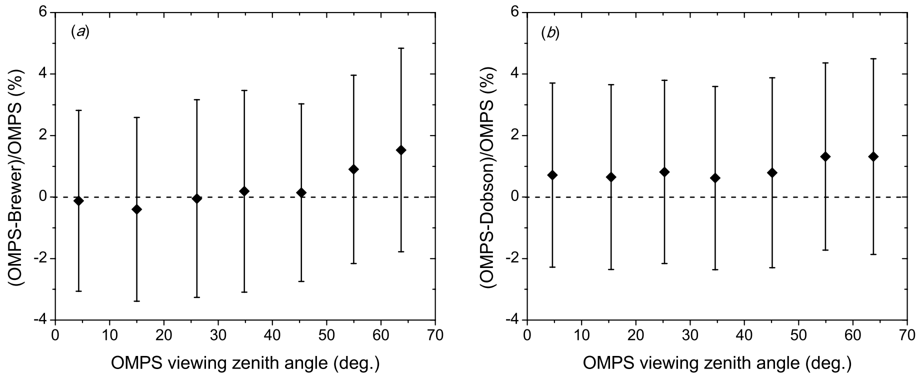

Fig. 6. Same as Fig. 5 but for OMPS viewing zenith angle.

AMTD
6, 4577–4605, 2013

Validation of the Suomi NPP Ozone Mapping and Profiler Suite total ozone

K. Bai et al.

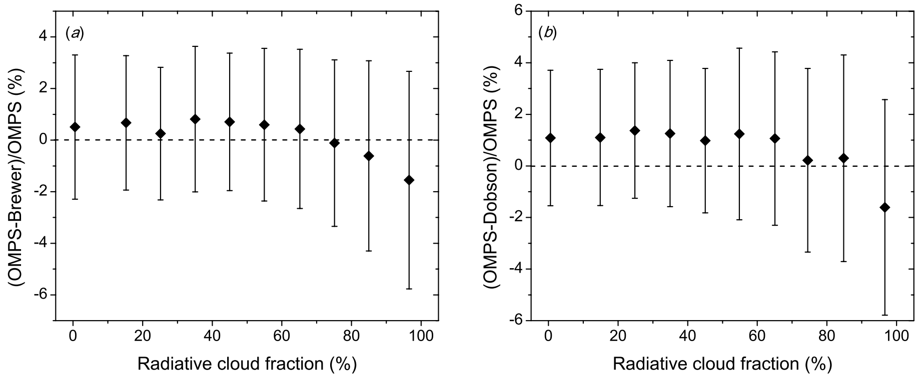

Fig. 7. Investigation of the bias error dependence on radiative cloud fraction.

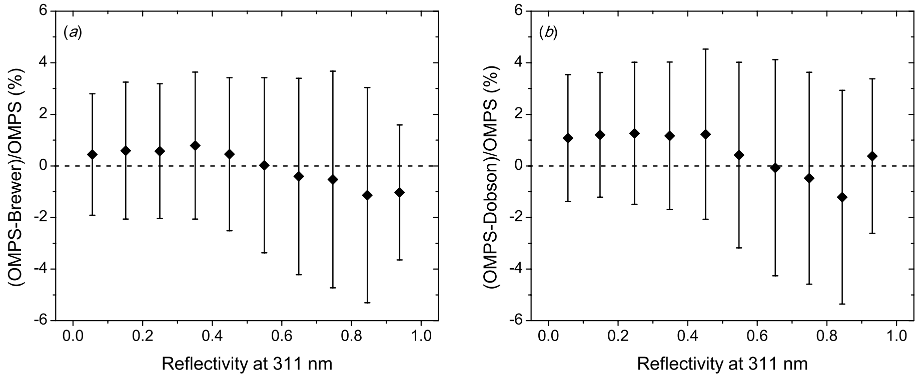

Fig. 8. Mean bias error against reflectivity at 311 nm.

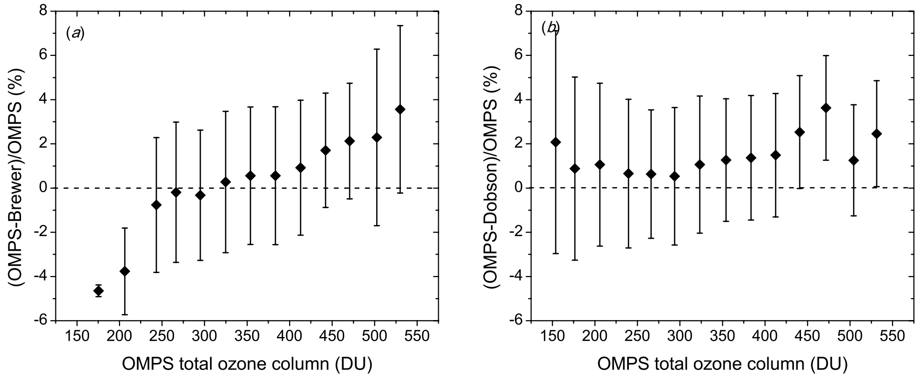

Fig. 9. Variation of bias error as a function of OMPS TC ozone value.

AMTD

6, 4577–4605, 2013

Validation of the Suomi NPP Ozone Mapping and Profiler Suite total ozone

K. Bai et al.

Title Page
Abstract Introduction
Conclusions References
Tables Figures
Back Close
Full Screen / Esc
Printer-friendly Version
Interactive Discussion